The May 2013 SNPP Cal/Val Campaign – Validation of Satellite Soundings

William Smith Sr[a,b], A. Larar[c], M. Goldberg[d], X. Liu[c], H. Revercomb[a], E. Weisz[a], M. Yesalusky[e], and D. Zhou[c]
[a]University of Wisconsin-Madison, Madison WI, USA, [b]SSAI / Langley Research Center, Hampton, VA, USA, [c]NASA Langley Research Center, Hampton VA, USA,
[d]NOAA/Nesdis, College Park, MD, USA, [e]Hampton University, Hampton VA, USA.

ABSTRACT

The NAST-I and SHIS ultra spectral interferometer sounders flew on the NASA ER-2 aircraft during the May 2013 S-NPP Calibration/Validation Campaign. The ER-2 under flew the Metop-A and -B, Aqua, and SNPP satellites, which carry the IASI, AIRS, and CrIS ultra spectral sounding instruments, respectively. Special ground truth radiosonde and surface based upward viewing ultra spectral radiance Planetary Boundary Layer (PBL) sounding observations (i.e., from the AERI and the ASSIST interferometer spectrometers) were obtained at the DOE Southern Great Plains (SGP) ARM CART-site and from a mobile ground site located in Yuma, Arizona. A common physical/statistical sounding retrieval algorithm and statistical database have been applied to the aircraft, ground-based interferometer, and satellite ultra spectral radiance data in order to use the higher spatial resolution aircraft data and higher vertical resolution surface-based interferometer PBL soundings, and radiosonde profiles, to validate the satellite sounding products. Differences between the satellite and the surface/airborne ground "truth" measurements are discussed. In particular, the comparisons between the satellite retrieved profiles and the ground truth observations revealed that improvements in the specification of surface emissivity spectra were needed in order to retrieve accurate atmospheric structure in the Planetary Boundary Layer (PBL). As a result a physical simultaneous surface skin/surface emissivity determination algorithm was implemented which improved the accuracy of atmospheric profiles retrieved throughput the lower troposphere. Here, special emphasis is given to validating the satellite atmospheric stability and time tendency observations made prior to the development of the devastating Moore, OK tornado on May 20, 2013.

Keywords: Ultra-spectral, hyper-spectral, satellites, meteorology, sounding, remote sensing

1. OBSERVATIONS AND ALGORITHMS

1.1 Observations

The Suomi National Polar-orbiting Partnership (SNPP) satellite Calibration/Validation Campaign was held during May 2013. The NASA high altitude (20-km) ER-2 aircraft, which carried the NAST-I and SHIS ultra-spectral interferometer sounders, flew under the Metop-A and -B, Aqua, and SNPP satellites, which carry the IASI, AIRS, and CrIS ultra-spectral sounding instruments, respectively. The primary motivation of the ultra-spectral sounding technique was to obtain high vertical resolution atmospheric temperature and moisture profiles needed for improving regional and global scale weather forecasts[1,2]. The horizontal scanning HIS (S-HIS) and the NASA / JPSS Atmospheric Sounder Testbed-Interferometer, (NAST-I) are flown on NASA aircraft to demonstrate the value of ultra-spectral resolution data for profiling the atmosphere and for validating the space borne ultra-spectral sounders currently in polar orbit[3]. The Atmospheric Infrared Sounder (AIRS)[3] on NASA's Aqua satellite was the first US experimental space demonstration of the technique and capability, while the first operational polar orbiting satellite implementation, Infrared Atmospheric Sounding Interferometer (IASI), was initiated on the European Metop-A and Metop-B satellites[4]. These sensors enable the spectral resolving power from 1000 to 10,000, respectively, providing the spectral resolution and signal to noise ratio needed to resolve temperature and water vapor profiles with a vertical resolution of 1-2 Km, depending on altitude. The first NOAA ultra-spectral sounder, the Cross-track Infrared Sounder (CrIS), was launched in 2011 on the Suomi-National Polar-orbiting Partnership (S-NPP) satellite[5]. The CrIS has the distinction of having the lowest noise level of any sounding instrument ever flown. The spectral coverage characteristics of the aircraft and satellite ultra-spectral sounding instruments discussed are shown in figure 1.

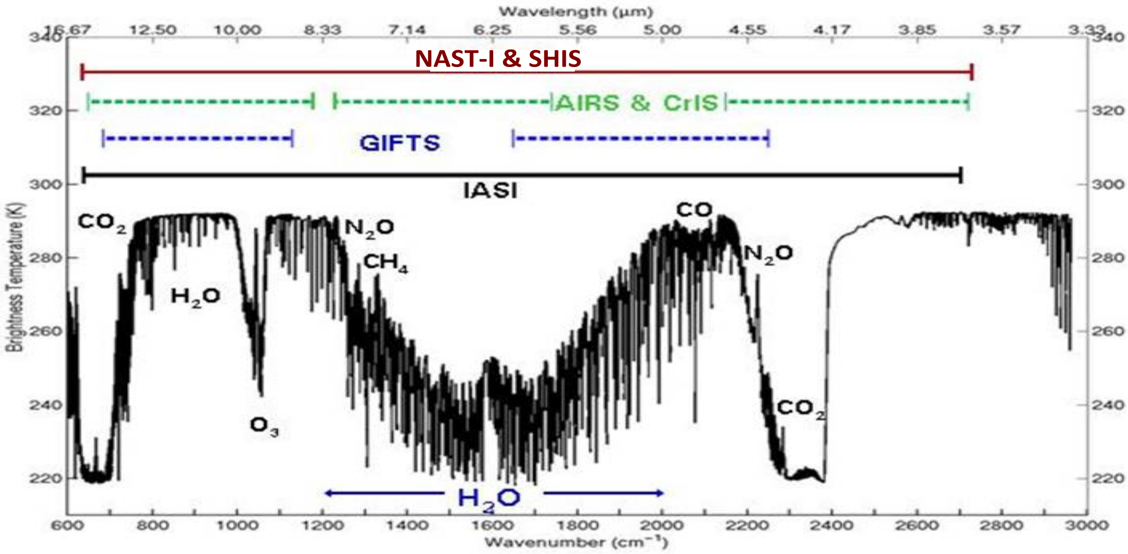

Figure 1. The IR spectra used for atmospheric sounding of the atmosphere and the regions used by some of the current ultra-spectral sounders.

Figure 2 shows the flight tracks of the NASA ER-2 during the SNPP cal/val campaign[6]. The flights over the ocean were conducted for CrIS radiance measurement calibration / validation. Flight tracks were chosen so as to achieve clear sky conditions over the thermally uniform ocean surface. The results of the CrIS radiance validation during the SNPP Cal/Val campaign are presented elsewhere[6,7]. For the CrIS sounder sounding accuracy and utility validation, flights were made over ground truth radiosonde and surface upward looking interferometer validation sites, one established at Yuma, AZ and the other being the ARM-CART site at Lamont, OK (figure 3). Both ground-truth sites were equipped with a surface weather station, a ground-based interferometer (AERI at the ARM-site[8] and ASSIST[9] for observing detailed structure of the PBL[10,11] and radiosonde observations. These surface weather, ground-based interferometer measurements, and radiosonde observations were combined with NOAA's Global Assimilation System (GDAS) model data to produce a "best estimate" of the atmospheric state at the time of the NASA ER-2 aircraft and satellite overpass measurements. Thus the retrieval validation data had the benefit of all the profile data available for the operational forecast system as well as the special research quality observations made at the Yuma, AZ and Lamont, OK ground sites.

1.2 Dual Regression Methodology

Ultraspectral infrared sounders measure the top-of-atmosphere radiance emitted by the Earth system with very high spectral resolution over a range of several thousand channels. The great advantage of high spectral resolution is an increased sensitivity to the vertical structure within the atmospheric column. The spectrum of relatively low vertical resolution infrared radiances can be de convoluted (i.e., inverted) to produce vertical profile information about the state of the atmosphere. Retrieval algorithms are designed to maximize the information content, minimize the propagation of noise, and retrieve the most probable atmospheric profile based on the observed radiance spectrum. The Dual-regression (DR) technique[12,13] retrieval algorithm, which has its origins with the airborne NAST-I sounding retrieval approach[14,15] utilizes physically simulated radiance based regression relations to produce atmospheric profiles and surface and cloud parameters at the full resolution of the sounding spectrometer. The DR linear regression ensures the processing speed necessary for real-time applications and includes geophysical classification and threshold tests to account for the non-linear dependence of infrared radiance on moisture and clouds. The DR method utilizes the full information of high-spectral resolution measurements (i.e., all the channels are used). In this application, trace gas profiles are also produced, including ozone, carbon monoxide, methane, and nitrous oxide. The chemistry profile results will be presented elsewhere. In the Suomi-NPP Calibration and Validation Campaign application discussed here, the Dual Regression statistics are produced using data from the Real-time Air Quality Modeling System (RAQMS), which outputs profiles of temperature, moisture, ozone, carbon monoxide, methane, and nitrous oxide[16]. A climatology consisting of the entire month of May over the central and western United States (20 – 40N, 95 – 125 W) for the year 2010 was used to generate radiance spectra, using PCRTM[17] and the regression statistics for each of the satellite and aircraft instruments whose radiances were used in the retrieval process.

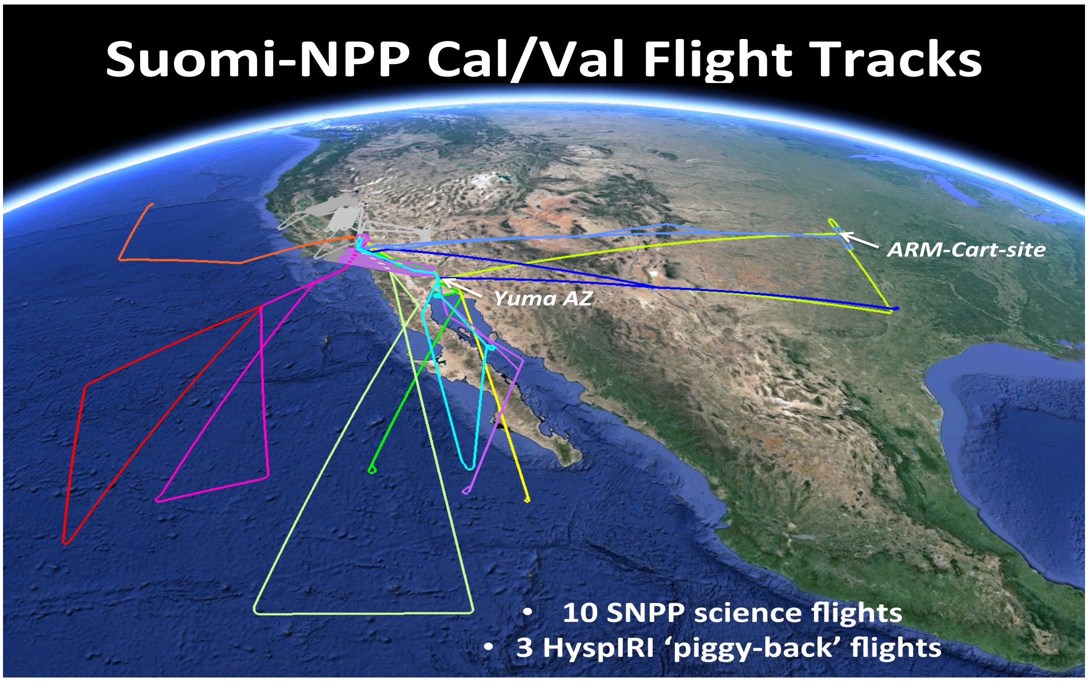

Figure 2. The NASA ER-2 flight tracks during the SNPP Cal/Val Campaign.

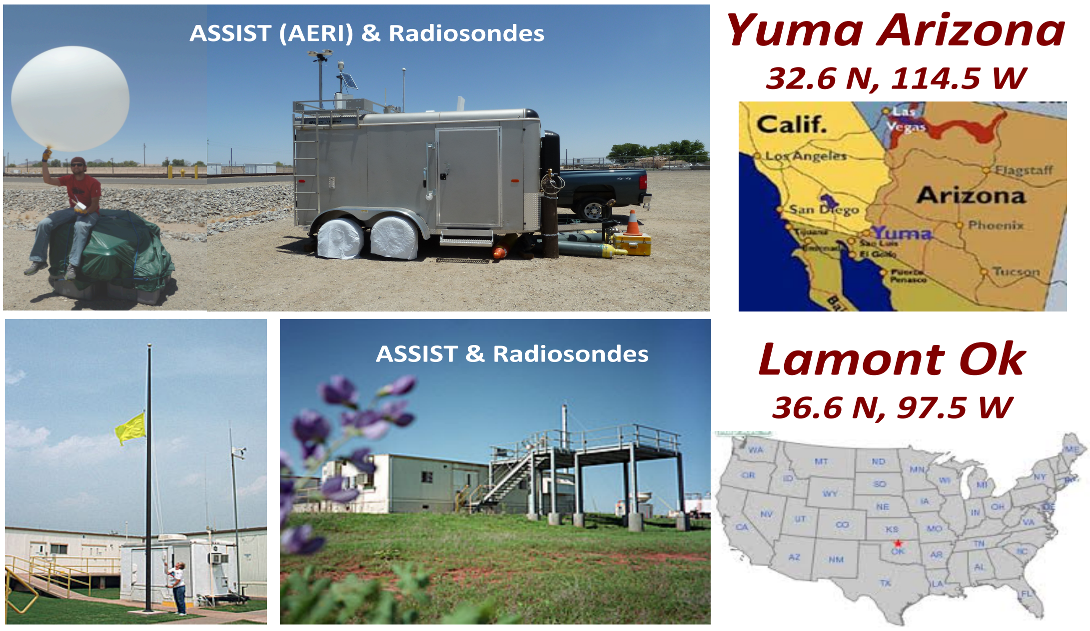

Figure 3. The SNPP Cal/Val Campaign surface ground-truth validation sites.

Surface Emissivity Correction: For this study PCRTM simulated radiances are used to derive the regression coefficients from a climatological data set assuming a “black (i.e., ε =1)” surface with the skin temperature equal to the air temperature. Thus, the observed radiances must be “corrected” for the real non-black skin/air temperature contrast surface condition. This is performed using an iterative scheme where the surface correction is performed using:

$$\mathbf{R_m\ (\varepsilon = 1;\ Ts = Ta\ ) = R_m\ (\varepsilon,\ Ts,\ Ta\ ) - [R_c\ (\varepsilon,\ Ts,\ Ta\ ) - R_c\ (\varepsilon = 1,\ Ts = Ta]}$$

where the calculated radiances are defined from an iterated guess atmospheric and surface state. The surface emissivity and skin temperature are determined using the “minimum emissivity variance” technique[18] where the sky radiance is calculated from the guess atmospheric state. The initial guess for this emissivity/skin temperature determination and radiance correction process comes from the operational GFS model.

The Yuma ground truth station is in the Arizona desert (see figure 3). For this non-uniform desert, there is a strong spectral and spatial variation of surface emissivity as can be seen from figure 4. In this figure is shown the mean and standard deviation of surface emissivity for the Arizona desert within a 50 km radius of Yuma, AZ (top panels) and the atmospheric temperature and moisture profile retrievals associated with them (bottom panels) on May 20, 2013. The red curves correspond to a climatological mean emissivity spectrum produced from four years of IASI data whereas the black curves correspond to the instantaneous emissivity spectra calculated from CrIS radiance spectra using the minimum emissivity variance algorithm described above. As can be seen from figure 4, there is a greater spectral and spatial variation in the surface emissivity than is represented by the climatological data. One can also see a much larger contrast between the surface air and surface skin temperature (i.e., 25 K) associated with the CrIS retrieved surface emissivity spectra than is calculated from the CrIS radiance spectra (21 K) assuming the climatological emissivity spectral values. The panels in the lower portion of figure 4 show that much better agreement between the CrIS retrieved temperature and water vapor profiles over Yuma (i.e., CrIS field of view center separation of 4 km from the Yuma ground station) is achieved with the ASSIST plus radiosonde profiles using the retrieved emissivity spectrum and associated surface skin temperature than is obtained using the climatological emissivity and associated surface skin temperature in the profile retrieval process. Figure 5 shows the ASSIST (plus Radiosonde) temperature and relative humidity cross- sections observed at the Yuma ground station on May 20, 2013 (upper panels). The lower panels show the CrIS retrievals with the ASSIST plus radiosonde (ASSIST) and radiosonde only profiles observed at 19 and 21 UTC on May 20, 2013. One can see from the ASSIST time cross-sections that there is a significant diurnal variation on the temperature and relative humidity within the PBL below the 3-km level. The ASSIST and CrIS temperature and humidity profiles observed at the SNPP overpass time (20.8 UTC) are in amazingly good agreement, whereas the radiosonde observations appear to be erroneously warm, possibly due to the sensors not stabilizing to the ambient air temperature fast enough as the balloon rise rapidly through the PBL. Above the PBL there is good agreement between the CrIS retrievals and the radiosonde observations.

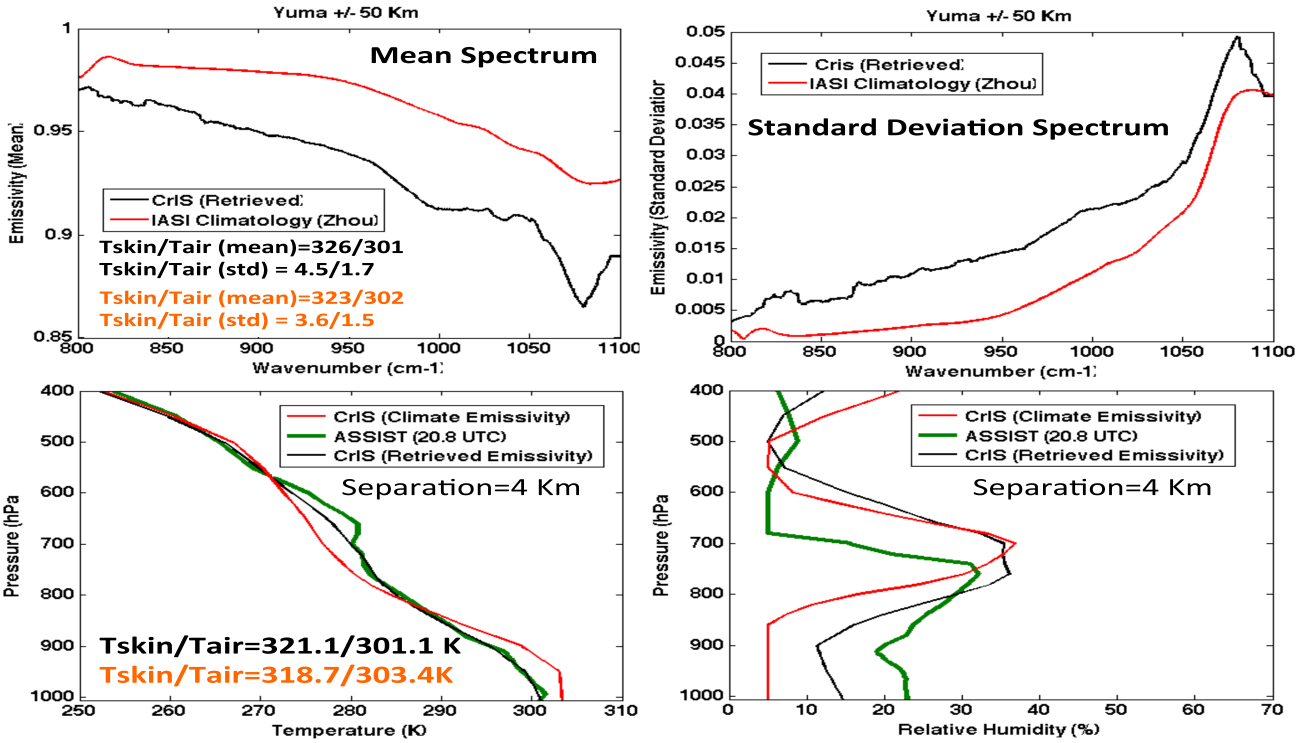

Figure 4. Mean and standard deviation of surface emissivity for the Arizona desert within a 50 km radius of Yuma AZ (top panels) and the atmospheric temperature and moisture profile retrievals associated with them (bottom panels) on May 20, 2013. The red curves correspond to a climatological mean emissivity spectrum produced from four years of IASI data whereas the black curves correspond to the instantaneous emissivity spectra calculated from CrIS radiance spectra using the minimum emissivity variance algorithm described here.

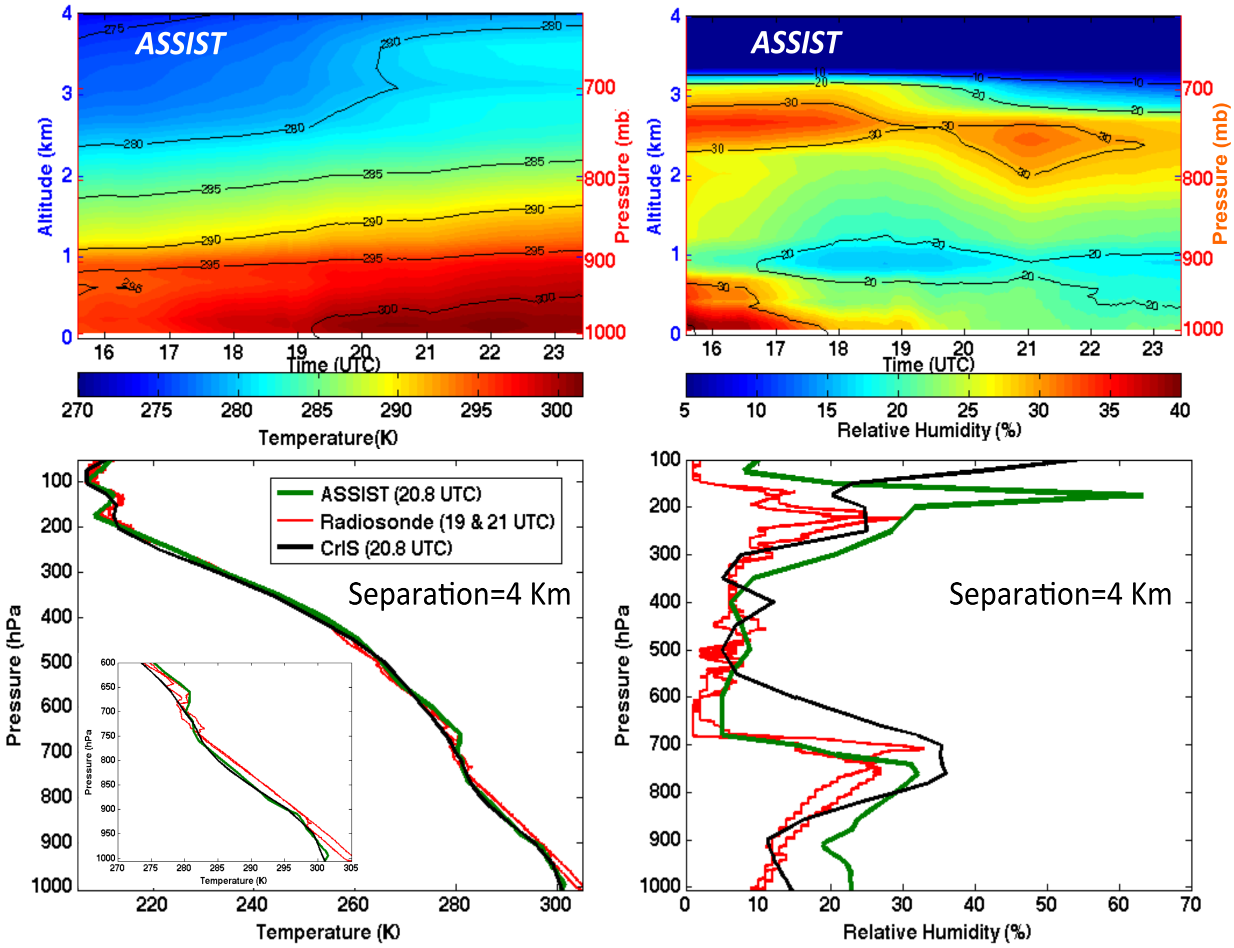

Figure 5. ASSIST (plus Radiosonde) temperature and relative humidity cross-sections observed at the Yuma ground station on May 20, 2013 (upper panels). The lower panels show the CrIS retrievals with the ASSIST plus radiosonde (ASSIST) and radiosonde only profiles observed at 19 and 21 UTC on May 20, 2013.

1.3 Statistical Bias Correction

A physical radiative transfer based adjustment to the DR retrieval is made on the basis of NOAA's 111-km resolution GDAS forecast model profile in order to eliminate the statistical bias in the retrieved profile vertical structure to the mean profile of the statistics used to formulate the regression retrieval coefficients. This physical adjustment is produced by computing the radiance spectrum from the forecast profile and producing a sounding retrieval from the calculated radiance spectrum, in exactly the same manner as that used with the real satellite measured radiance spectrum. The difference between the simulated radiance retrieval and the forecast profile is the retrieval bias due to the imperfect skill of the statistical regression relationships. This retrieval bias is removed from the real satellite radiance profile retrieval. Figure 6 shows a comparison between an IASI retrieval with (Bias Corrected) and without (i.e., regression) the retrieval bias removal with a nearby radiosonde observation. As can be seen the finer scale vertical structure shown by the radiosonde that is not captured in the regression retrieval is captured in the bias corrected retrieval.

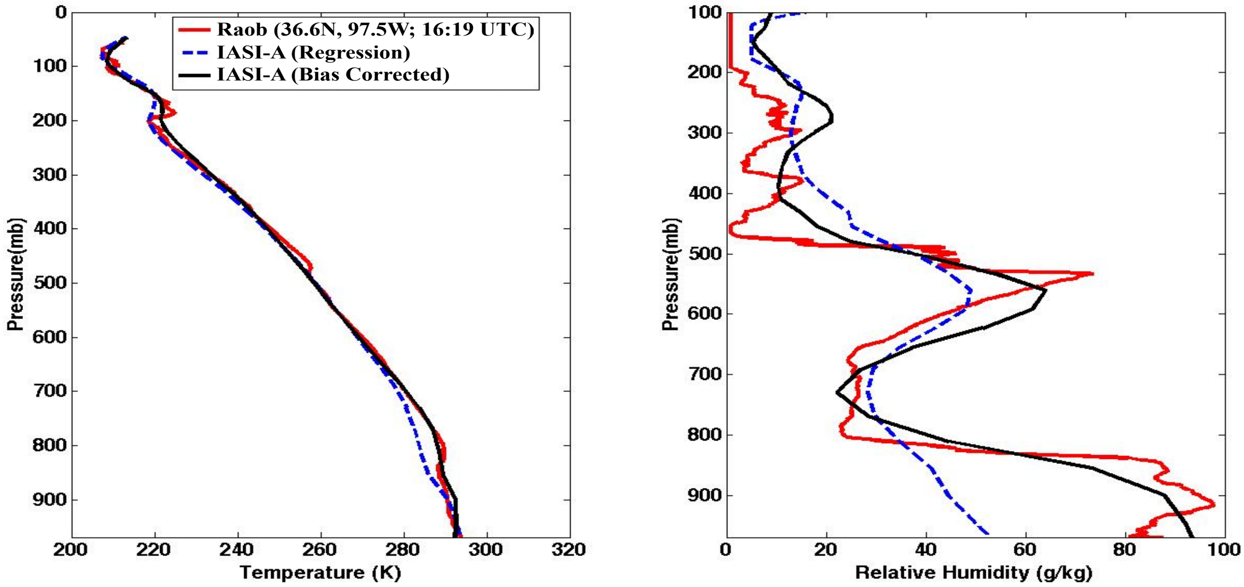

Figure 6. Comparison between an IASI retrieval at 15:56 UTC obtained with (i.e., Bias Corrected) and without (i.e., regression) the retrieval bias adjustment with a nearby radiosonde observation at the ARM CART-site at 16:19 UTC.

2. TORNADO CASE STUDY

2.1 May 20 , 2013 Oklahoma Tornado Validation Flight

On May 20, an ER-2 validation flight was flown from Palmdale, California to Oklahoma in order to validate CrIS soundings associated with a forecasted severe weather outbreak. The flight track is shown in yellow on figure 2. A special radiosonde observation at the DOE ARM-site in Lamont, Oklahoma was scheduled for the time of the SNPP overpass time. During the flight mission a deadly EF-5 tornado developed one hour after the SNPP satellite overpass near Moore Oklahoma to the south of the ARM-site. Figure 7 shows the ground tracks of the Metop-A, Metop-B, SNPP, an Aqua satellite overpasses, which occurred before and during the initiation of the severe weather outbreak. Metop-A, Metop-B, and SNPP observed the atmospheric conditions about four, three, and one hour before the severe weather occurrence, while Aqua observed the atmospheric conditions at the time of the severe weather outbreak. The Moore, OK tornado, which occurred about 20 UTC, killed 24 people and destroyed approximately 2300 houses. Figure 8 shows the SNPP CrIS "window" channel (950 – 1000 cm^{-1}) brightness temperature observed for the Oklahoma / Texas region. The rectangular outline around Moore, OK illustrates the mesoscale region for which the soundings derived from the satellite and aircraft data are shown in subsequent figures. The stared circle denotes the location of Moore, OK. It can be seen from the brightness temperature values that the convection associated with the Moore tornado had already been initiated south of Moore at the time of the SNPP overpass.

For a tornado to develop low-level moisture, atmospheric instability resulting from warm moist air lying beneath cold dry air aloft, and a lifting mechanism must exist. The thermodynamics and dynamics act together with warm moist air within the boundary layer converging into an area where there is the advection of cold dry air aloft, as associated with a cold front or a dry line. Such dry lines are common in the central plains region of the United States where dry air from the North or West meets warm moist air moist moving northward from the Gulf of Mexico. Typically, the convection is initially suppressed by a temperature inversion produced by nocturnal cooling and associated subsidence. Once the nocturnal "moisture capping" inversion erodes due to daytime surface heating, the warm air rises rapidly as an updraft and produces the thunderstorm. Some of the most violent tornadoes develop from super cell thunderstorms, which are characterized by persistent rotating updrafts of air. The jet stream adds yet more energy to this development. On May 20th the weather conditions of warm moist air convergence under cold dry air along a frontal boundary combined over central Oklahoma with strong wind shear due to the presence of a jet stream to produce a violent tornado outbreak.

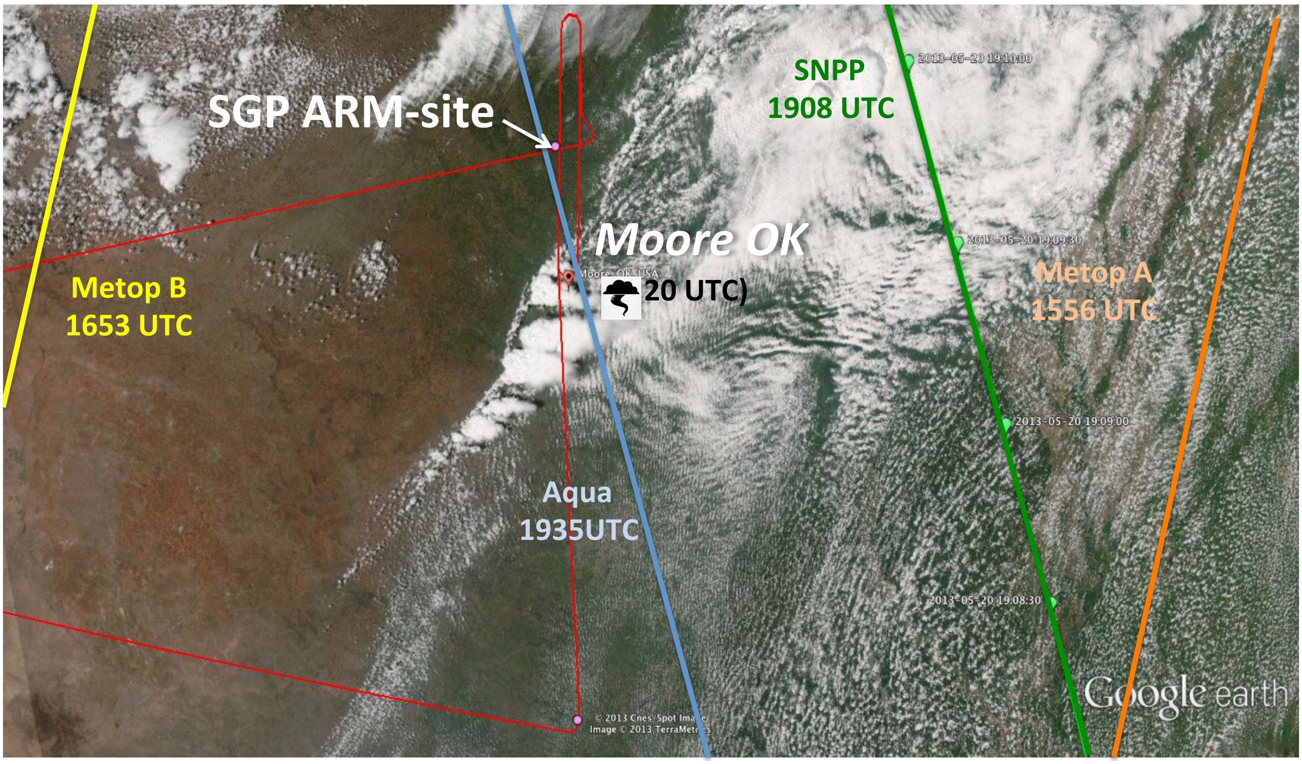

Figure 7. Satellite orbits and ER-2 flight tracks over the Oklahoma region, which experienced severe weather on 20 May 2013.

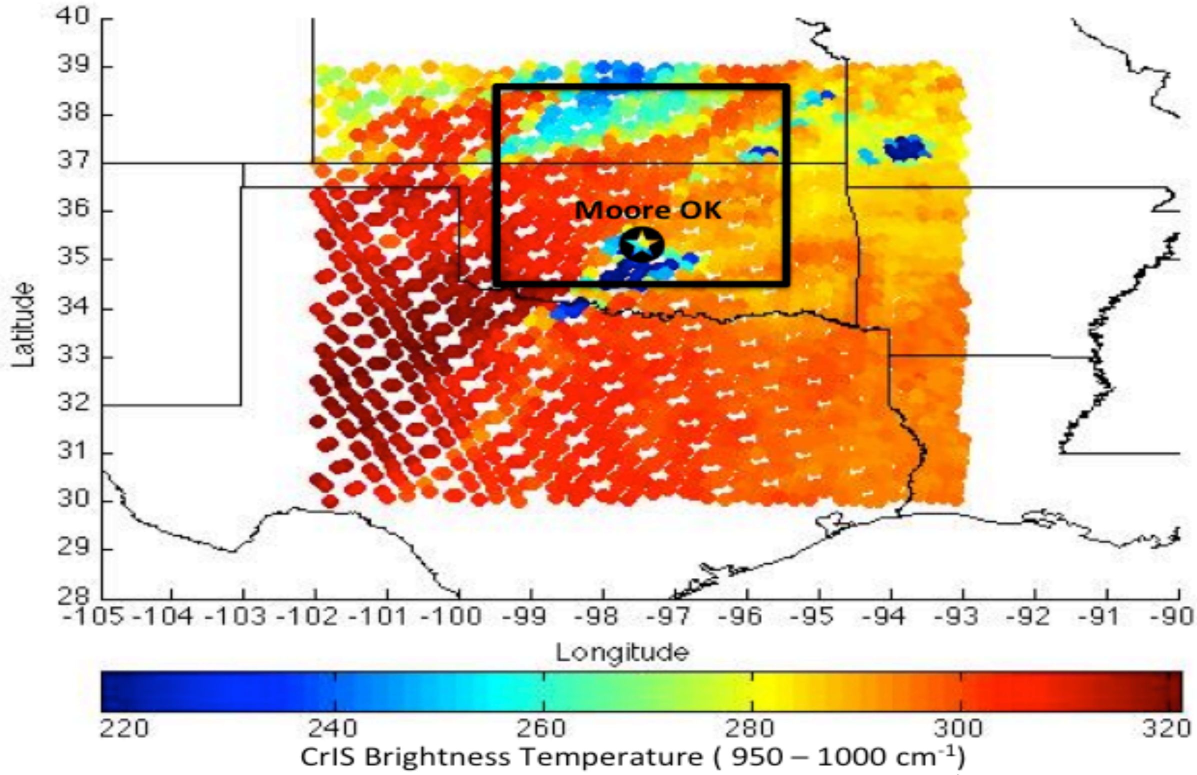

Figure 8. SNPP CrIS observed brightness temperature for the spectral region 950 – 1000 cm^{-1}. The rectangular outline illustrates the geographical area for which subsequent figures are shown.

The main variable presented here was the Lifted Index (LI) stability parameter, which is derived from the retrieved temperature and moisture soundings. The lifted index is a measure of the buoyancy of the atmosphere. Decreasing values of LI indicate destabilizing conditions an increasing probability of convective storm development. Negative values of LI indicate unstable atmospheric conditions with LI values below -5 indicative of a high probability for strong thunderstorm development.

Figure 9 shows the LI values obtained from the DR retrievals from IASI-A (upper left panel), IASI-B (upper right panel), CrIS (lower left panel), and AIRS (lower right panel), which clearly show how the stability of the atmosphere decreased dramatically over Oklahoma during the morning and early afternoon hours of 20 May 2013. The tornado symbol on each panel denotes the location of Moore, OK. These CrIS and AIRS observations, which were obtained one hour and one-half hour before the Moore Tornado show extreme negative LI values in the vicinity of Moore, OK. The white areas of these images show that (infrared) soundings could not be obtained down to the surface directly over Moore because of the heavy cloud cover generated by the convection initiated just prior to the SNPP overpass.

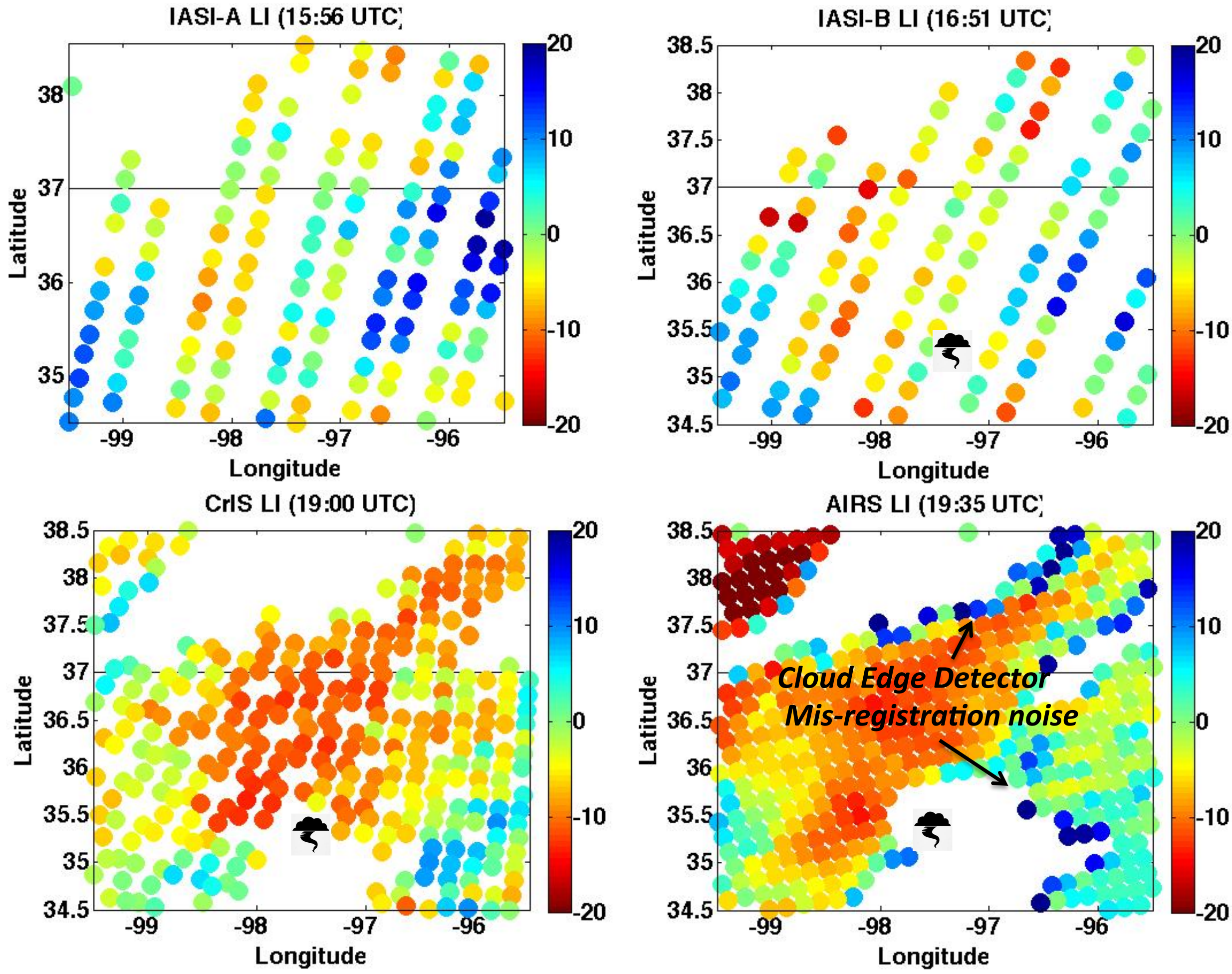

Figure 9. LI values obtained from IASI-A (upper left panel), IASI-B (upper right panel), CrIS (lower left panel), and AIRS (lower right panel).

3. SUMMARY AND CONCLUSIONS

CrIS soundings can be validated using ASSIST/AERI and radiosonde data obtained at the Yuma, AZ and Lamont, OK (ARM) SNPP ground truth sites. It is shown that for desert locations (e.g., Yuma, AZ) the accuracy of the retrieval in the lower troposphere is highly dependent on the accuracy of surface emissivity specification. CrIS retrievals obtained using a physical retrieval of surface emissivity and skin temperature compare well with radiosonde and ASSIST/AERI ground truth measurements obtained at the SNPP ground truth sites. Satellite soundings provide mesoscale features useful for delineating where convection and severe weather will occur.

REFERENCES

[1] Smith, W. L., "Atmospheric soundings from satellites - false expectation or the key to improved weather prediction?" Quarterly Journal of the Royal Meteorological Society, 117, 267-297 (1991)
[2] Smith, Sr., W.L. H. Revercomb, G. Bingham, A. Larar, H. Huang, D. Zhou, J. Li, X. Liu, and S. Kireev, "Evolution, current capabilities, and future advances in satellite ultra-spectral IR sounding" Atmos. Chem. Phys., 9, 6541-6569 (2009)
[3] Chahine, M.T., and co-authors, "AIRS: Improving Weather Forecasting and Providing New Data on Greenhouse Gases" *Bull. Amer. Meteor. Soc.*, 87, 911-926 (2006)
[4] Hilton, Fiona, and Coauthors, "Hyperspectral earth observation from IASI: five years of accomplishments" *Bull. Amer. Meteor. Soc.*, 93, 347–370 (2012).
[5] Tobin, David and co-authors, "Suomi-NPP CrIS radiometric calibration uncertainty" .J. Geo. Res.-Atm., 118, (2013).
[6] Taylor, J. K., D. C. Tobin, H. E. Revercomb, F. A. Best, R. O. Knuteson, R. K. Garcia, D. Deslover, and L. A. Borg "Suomi NPP/JPSS Cross-track Infrared Sounder (CrIS): Calibration Validation With The Aircraft Based Scanning High-resolution Interferometer Sounder (S-HIS)" 10th Annual Symposium on New Generation Operational Environmental Satellite Systems, 94th American Meteorological Society Annual Meeting, Atlanta Georgia, February 2-6, (2014)
[7] Larar, A. M., W.L. Smith Sr., D. Zhou, X. Liu, and J. J. Tian "The Suomi NPP airborne field campaign and preliminary NAST-I radiance results" 19th International TOVS Study Conference, Jeju Island, South Korea, 26 March – 1 April, (2014)
[8] Knuteson, R. O., H. E. Revercomb, F. A. Best, N. C. Ciganovich, R. G. Dedecker, T. P. Dirkx, S. C. Ellington, W. F. Feltz, R. K. Garcia, H. B. Howell, W. L. Smith, J. F. Short, and D. C. Tobin "Atmospheric Emitted Radiance Interferometer, Part I: Instrument design" J. Atm. Oceanic Tech., 21, 1763-1776 (2004)
[9] Rochette, W. L. Smith Sr., M. Howard, and T. Bratcher "ASSIST Atmospheric Sounder Spectrometer for Infrared Spectral Technology-latest development and improvement in the atmospheric sounding technology" Imaging Spectrometry XIV Proceedings of SPIE, 7457, 50-60 (2009)
[10] Feltz, W F., W. L. Smith, R. O. Knuteson, H. E. Revercomb, H.M. Woolf, and H. B. Howell "Meteorological Applications of Temperature and Water Vapor Retrievals from the Ground-Based Atmospheric Emitted Radiance Interferometer (AERI)" *J. Appl. Meteor.* 37, 857–875 (1998)
[11] Smith, W. L., W. F. Feltz, R. O. Knuteson, H. E. Revercomb, H.M. Woolf, and H. B. Howell, "The retrieval of planetary boundary layer structure using ground-based infrared spectral radiance measurements" J. Atm. Oceanic Tech., 16, 323-333 (1999)
[12] Smith Sr., W. L., E. Weisz, S. Kireev, D. K. Zhou, Z. Li, and E. Borbas "Dual-regression retrieval algorithm for real-time processing of satellite ultraspectral radiances" Journal of Applied Meteorology and Climatology, 51, 1455–1476 (2012)
[13] Weisz, E., W. L. Smith Sr., and N. Smith, "Advances in simultaneous atmospheric profile and cloud parameter regression based retrieval from high-spectral resolution radiance measurements" *J.Geo.Res.*, 118, 6433-6443 (2013)
[14] Zhou, D. K.; W. L. Smith, J. Li, H. B. Howell, G. Cantwell, A. Larar, R. O. Knuteson, D. C. Robin, H. E. Revercomb, and S. Mango "Thermodynamic product retrieval methodology and validation for NAST-I" Applied Optics, 41, 6957-6967 (2001)
[15] Smith Sr., W. L., D. K. Zhou, A. M. Larar, S. A. Mango, R. O. Knuteson, H.E. Revercomb, and W. L. Smith Jr., "The NPOESS Airborne Testbed Interferometer – Remotely Sensed Surface and Atmospheric Conditions during CLAMS" J. Atmos. Sci., 62, 1118–1134 (2005)
[16] Pierce, R. B., and co-authors "Regional Air Quality Modeling System (RAQMS) predictions of the tropospheric ozone budget over east Asia" *J.Geo.Res.*, 108, 1984-2012 (2003)
[17] Liu, Xu, Smith, W. L.; Zhou, D.K. and A. Larar "Principal component-based radiative transfer model for hyperspectral sensors-Theoretical concept" Applied Optics, 45, 201-209 (2006)
[18] W. Smith, L. West, G. Gimmestad, and S. E. Lane, "Ultra-spectral measurements of surface emissivity with an imaging interferometer spectrometer," Hyperspectral Imaging and Sounding of the Environment, OSA Technical Digest, Optical Society of America (2011)

Acknowledgements
The authors acknowledge the financial support of NASA and NOAA, and the DOE for their support of this research. The support of Michael Howard (NSTech) for providing the ASSIST instrument for the Yuma ground validation site is gratefully acknowledged.